HHS Public Access

Author manuscript

Metabolomics. Author manuscript; available in PMC 2017 April 01.

Published in final edited form as:

Metabolomics. 2016 April ; 12(4): . doi:10.1007/s11306-016-0998-5.

Guinea pig genital tract lipidome reveals in vivo and in vitro regulation of phosphatidylcholine 16:0/18:1 and contribution to *Chlamydia trachomatis* serovar D infectivity

Shradha Wali[1], **Rishein Gupta**[1], **Jieh-Juen Yu**[1], **Adelphe Mfuh**[2], **Xiaoli Gao**[3], **M. Neal Guentzel**[1], **James P. Chambers**[1], **Sazaly Abu Bakar**[4], **Guangming Zhong**[5], and **Bernard P. Arulanandam**[1]

Bernard P. Arulanandam: bernard.arulanandam@utsa.edu

[1]South Texas Center for Emerging Infectious Diseases and Center for Excellence in Infection Genomics, University of Texas at San Antonio, One UTSA Circle, San Antonio, TX 78249, USA

[2]Department of Chemistry, University of Texas at San Antonio, One UTSA Circle, San Antonio, TX 78249, USA

[3]Department of Biochemistry, University of Texas Health Science Center at San Antonio, San Antonio, TX 78229, USA

[4]Department of Medical Microbiology, Faculty of Medicine, University of Malaya, Lembah Pantai Kuala Lumpur, 50603 Kuala Lumpur, Malaysia

[5]Department of Microbiology and Immunology, University of Texas Health Science Center at San Antonio, 7702 Floyd Curl Drive, San Antonio, TX 78229, USA

Abstract

Introduction—*Chlamydia trachomatis* (Ct), is the leading cause of sexually transmitted infections worldwide. Host transcriptomic- or proteomic profiling studies have identified key molecules involved in establishment of Ct infection or the generation of anti Ct-immunity. However, the contribution of the host metabolome is not known.

Objectives—The objective of this study was to determine the contribution of host metabolites in genital Ct infection.

Methods—We used high-performance liquid chromatography-mass spectrometry, and mapped lipid profiles in genital swabs obtained from female guinea pigs at days 3, 9, 15, 30 and 65 post Ct serovar D intravaginal infection.

Correspondence to: Bernard P. Arulanandam, bernard.arulanandam@utsa.edu.

Shradha Wali and Rishein Gupta have contributed equally.

Electronic supplementary material The online version of this article (doi:10.1007/s11306-016-0998-5) contains supplementary material, which is available to authorized users.

Compliance with ethical standards

Ethical approval All Authors listed in this manuscript agree and comply with compliance with ethical requirements.

Conflict of Interest The authors have no conflicts of interest to declare in regards to this work.

Results—Across all time points assessed, 13 distinct lipid species including choline, ethanolamine and glycerol were detected. Amongst these metabolites, phosphatidylcholine (PC) was the predominant phospholipid detected from animals actively shedding bacteria i.e., at 3, 9, and 15 days post infection. However, at days 30 and 65 when the animals had cleared the infection, PC was observed to be decreased compared to previous time points. Mass spectrometry analyses of PC produced in guinea pigs (in vivo) and 104C1 guinea pig cell line (in vitro) revealed distinct PC species following Ct D infection. Amongst these, PC 16:0/18:1 was significantly upregulated following Ct D infection ($p < 0.05$, >twofold change) in vivo and in vitro infection models investigated in this report. Exogenous addition of PC 16:0/18:1 resulted in significant increase in Ct D in Hela 229 cells.

Conclusion—This study demonstrates a role for host metabolite, PC 16:0/18:1 in regulating genital Ct infection in vivo and in vitro.

Keywords

Guinea pig; *Chlamydia trachomatis* serovar D; Intravaginal infection; Lipids; Phosphatidylcholine

1 Introduction

Chlamydia trachomatis (Ct) is the leading cause of bacterial sexually transmitted infections worldwide and the most commonly reported notifiable disease in the U.S. (Adekoya et al. 2015; Torrone et al. 2014). Untreated genital Ct infection may lead to reproductive sequelae including cervicitis, pelvic inflammatory disease (PID), and infertility in women (Hafner 2015; Mascellino et al. 2011). Direct health care costs associated with Ct infection is estimated to be >$500 million annually (Owusu-Edusei et al. 2013, 2015), and with significant increasing annual incidence rates, intervention strategies are required (Gottlieb et al. 2014; Huston et al. 2012; Ozolins et al. 2013).

To improve approaches for efficient intervention and cure (Lyons et al. 2009; Hafner et al. 2014; Lal et al. 2013), a better understanding of chlamydial pathogenesis is required (Deruaz and Luster 2015; Vasilevsky et al. 2014). To this end, new insight(s) on pathogen-host interaction have been obtained from recent ‘global-profiling’ of *Chlamydia*- and host-specific factors (Brotman et al. 2014; Brunham and Rappuoli 2013). Transcriptome-wide or sequencing approaches have revealed the role for specific immune genes and associated pathways following infection with Ct-plasmid-sufficient and -deficient strains (Porcella et al. 2015; Carlson et al. 2008; Ferreira et al. 2013; Qu et al. 2015). Similarly, regulatory genetic species, namely microRNAs of bacterial and host origin have revealed the role(s) in growth and cellular function following infection (Derrick et al. 2013; Furuse et al. 2014; Gupta et al. 2015; Yeruva et al. 2014; Igietseme et al. 2013). Proteomic studies have identified immunodominant, T- and B cell chlamydial antigens involved in primary infection and vaccination (Cruz-Fisher et al. 2011; Wang et al. 2010; Karunakaran et al. 2015; Picard et al. 2012). Additionally, quantitative and semi-quantitative proteomic studies in human and murine cell lines have identified key ‘host-specific signatures’ associated with stress, inflammation, and pathogenesis (Kokes et al. 2015; Saka et al. 2015). In this regard, reports on the lipid droplet proteome in Ct L2 infected murine embryonic fibroblast cells (Saka et al.

2015), and the chlamydial inclusion interactome (Mirrashidi et al. 2015), provide new information on factors involved in chlamydial infectivity.

Despite these '*omics*'- based studies, there is minimal information on host-metabolite regulation in genital Ct infection. Using a general metabolomics approach, Muller et al., have reported a molecular cartograph of *C. pneumoniae* infected HEp2 cells, and supporting the role of previously non-annoted metabolites as biomarkers for infection (Muller et al. 2013). Nutrient requirements, maintenance of respiratory activity and metabolism of D-glucose in elementary bodies (EB) of the amoeba symbiont, *Protochlamydia amoebophila* has been demonstrated using metabolomics approaches (Sixt et al. 2013). Using a high-performance liquid chromatography–mass spectrometric method (HPLC–MS/MS), we examined the genital lipidome profile of Ct serovar D infected female Dunkin Hartley guinea pigs. We detected 13 lipids including choline, ethanolamine and glycerol to be most prevalent in swabs collected from infected guinea pigs. phosphatidylcholine (PC), and the precursor phosphotidyl-ethanolamine (PE) were most prevalent lipids (at 3, 9 and 15 days post infection) which were reduced 30 and 65 days *post* infection. We observed PC16:0/18:1 fatty acid following Ct D infection ($p < 0.05$, > twofold change) to be a common PC species regulated in guinea pigs and guinea pig cell line, 104C1. Consistent with our in vivo data, exogenous addition of PC 16:0/18:1 to Hela 229 and 104C1 cells exhibited increased bacterial infectivity suggesting a role for these host metabolites in Ct D genital infection.

2 Materials and methods

2.1 Bacteria

Chlamydial stocks were prepared as previously described (Li et al. 2013). Ct D EB (infectious form) were harvested from infected HeLa cells and stored at −80 °C in sucrose-phosphate-glutamine (SPG) buffer (pH = 7.4). Ct D preparations were titered and diluted appropriately for intra-vaginal (i.vag) infection.

2.2 Guinea pigs

Dunkin Hartley strain guinea pigs (350–450 g) were purchased from Charles River Laboratories (Massachusetts, USA) and housed in an AAALAC-accredited vivarium. Food and water were supplied ad libitum and all experimental studies were carried out under the aegis of the Guide for the Care and Use of Laboratory Animals of the National Institutes of Health. Protocol (IS0146) was approved by the Institutional Animal Care and Use Committee (IACUC) of the University of Texas at San Antonio.

2.3 Infection in guinea pigs

For sustained Ct D infection in guinea pigs, all animals received a subcutaneous injection of 5 mg β-estradiol (Sigma) in 100 μl sesame oil (Sigma) on days −10 and −3 prior to infection as described by de Jonge et al. (de Jonge et al. 2011). All guinea pigs were anesthetized with 3 % isoflurane before immunization and challenge procedures. Following infection with Ct D, vaginal swabs were collected at 4-day interval for 36 days from all guinea pigs and plated onto HeLa cell monolayers to determine the chlamydial burden as previously described (Li et al. 2008). Briefly, Ct D inclusion forming units (IFUs) were detected at 48 h using an anti-

Chlamydia genus specific rabbit monoclonal primary antibody, and goat anti-rabbit IgG secondary antibody conjugated to FITC plus Hoescht nuclear stain.

2.4 Genital tract pathology

Genital tract tissues were harvested on day 65 post-infection, fixed in 10 % formalin, embedded in paraffin, sectioned, and stained with hematoxylin-eosin (H&E). Histological images were obtained at ×200 or ×400 magnifications using an Olympus AX80 light microscope (Olympus, Center Valley, PA) and evaluated in a blind fashion for pathological damage (Wali et al. 2014). The microscopic findings were either graded as follows: none/minimal (0), slight (1), moderate (2), or severe (3) histological alteration. Histological scores were obtained by examination of five consecutive sections (2 mm) of cervix, oviduct, and uterus from every animal. Scores assigned to individual guinea pigs were used to calculate the pathology score for each group of animals and presented as mean ± standard deviation.

2.5 Lipidome analyses

2.5.1 Sample collection—*In vivo* Following infection with Ct D, vaginal swabs using applicators (Peel Pouch Dryswab™ ENT, MWE, Wiltshire, England) were collected at days 3, 9, 15, 30 and 65 post infection from guinea pigs. Swabs were collected from mock infected guinea pigs at each time point to serve as controls. All samples were snap frozen in dry ice and stored at −80 °C till further processing.

In vitro 104C1 guinea pig fetal cell line, kind gift from Dr. Roger Rank (Arkansas Children's Hospital Research Institute, Little Rock, AR), were cultured in 24 well plates at cell densities of 5×10^5 cells/well in D-10, DMEM supplemented with 10 % FBS (Gibco). 104C1 cells were infected in triplicate with Ct D at multiplicity of infection (0.05) and at 48 h post infection, removed using cell scrappers, washed twice with phosphate buffered saline (PBS) and stored at ×80 °C until used.

2.5.2 Sample processing—Lipids were extracted from swabs and cells as previously described (Gao et al. 2012). Briefly, five volumes cold (−20 °C) chloroform/methanol (2:1, v/v) was added per sample volume. Following thorough mixing (vortexing twice for 10 s), the extraction mixture was allowed to stand on ice for 10 min. Following centrifugation at ~ 13,800×g for 10 min, the chloroform layer was removed by pipetting and dried in vacuo. Prior to LC–MS analysis, the lipid extracts were reconstituted in 200 μl of isopropanol containing 10 mM ammonium acetate.

2.5.3 High-performance liquid chromatography–mass spectrometry and data processing—HPLC–MS/MS analyses were conducted on a Thermo Fisher Q Exactive fitted with a PicoChip nanospray source (New Objective). HPLC conditions were: column, Pico-Chip (Waters Atlantis dC18; 150 μm × 105 mm; 3 μm particle); mobile phase A, acetonitrile/water (40:60) containing 10 mM ammonium acetate; mobile phase B, acetonitrile/isopropanol (10:90) containing 10 mM ammonium acetate; gradient, 10 % B for 7 min (sample loading), 10–99 % B over 33 min, 99 % B for 15 min; flow rate, 1 μl/min. Data-dependent analyses were conducted using one full MS scan (70,000 resolution, *m/z* 300) followed by six tandem-MS scans. SIEVE (Thermo Fisher) was used to process the raw

data files. Peak alignment and integration was performed and the relative abundance was generated for each lipid among the different experimental groups. Lipid species were identified using LipidSearch (Thermo Fisher) and by searching the following databases: METLIN (http://metlin.scripps.edu/index.php) and LIPID MAPS (http://www.lipidmaps.org/data/structure/) using a 5-ppm mass tolerance. The putative lipid identifications were manually verified through examination of the tandem mass spectra and in comparison with the retention times from commercially available standards (Avanti Polar Lipids). Total metabolite abundance was used for normalization of samples using Progenesis CoMet software (Durham, NC).

In order to determine the most abundantly detected species of lipids, we compared the relative abundance of each detected lipid in swab samples obtained from Ct infected and uninfected guinea pigs. Lipids found to be twofold or greater in the ratio of Ct D infected compared to mock infected animals (Ct D/mock infected) at each time point (days 3, 9, 15, 30 and 65) were included in the study. The pie diagram profile (Fig. 2) for each time point was prepared by obtaining the percentage of each lipid. For example, PC percentage at day 3 was calculated as = (number of PC found to be > twofold at day 3/total number of > twofold lipids detected at day 3) × 100.

2.6 PC 16:0/18:1 and Ct D Infection

Phospholipid, 1,2-distearoyl-*sn*-glycero-3-phosphocholine (DSPC), 1,2-dioleoyl-*sn*-glycero-3-phosphoethanolamine-*N*-(carboxyfluorescein) (ammonium salt), L-α-phosphotidylglycerol sodium salt (FITC-PC) and PC 16:0/18:1 was commercially obtained (Avanti Polar Lipids, Inc., Alabaster, Al). Cholesterol was purchased from Calbiochem (San Diego, CA, USA). Liposome formulations were prepared by lipid film hydration and sonication methods as described previously (Mfuh et al. 2011; Li et al. 2012a, b). Liposome encapsulated PC 16:0/18:1 or liposomes alone were introduced into Hela and 104C1 cells in triplicate at a concentration of 25 μM/well. Following centrifugation at ~1000×g for 60 min at 25 °C, cells were washed with D-10 and infected with Ct D as described above.

2.7 Statistical analyses

The number of replicates for the in vivo and in vitro studies were 2 and 3 respectively. Student's *t* test was used for comparison between Ct D (n = 5) and mock infected (n = 3) groups. Differences were considered statistically significant if *p* values were <0.05 and obtained *p* values are noted in figures. All statistical analyses were conducted using the GraphPad Prism 5 software package (La Jolla, CA).

3 Results

3.1 *Chlamydia trachomatis* serovar D leads to distinct profiles of lipids following infection

Chlamydia caviae is the naturally infecting strain in guinea pigs and has been used by several laboratories to study chlamydial infection (Rank et al. 2003; Wali et al. 2014; Neuendorf et al. 2015). However, given that Ct D and Ct E are strains infecting humans, the translational value of the guinea pig model has further increased by the report of de Jonge et al. on establishment of Ct D and Ct E infection in guinea pigs (de Jonge et al. 2011). Using a

similar model system, we observed guinea pigs (n = 5) exhibited increased levels of Ct D shedding initially from days 4–8 (85,006 ± 46,401 IFU–58,162 ± 15,106 IFU), progressively decreasing (up to day 28: 3693 ± 2485 IFU) with complete clearance of infection (no detectable bacterial shedding) after day 28 (Fig. 1a). Ct infection resulted in tubal dilatation and upper genital tract pathology in infected animals. Specifically, genital tissue sections at day 65 post challenge exhibited moderate to severe congestion, hemorrhage, and edema accompanied with severe infiltration of inflammatory cells (lymphocytes and neutrophils) within the oviducts (Fig. 1b). In order to determine lipid signatures associated with Ct infectivity, genital swabs were collected at five different intervals representative of "phases" of guinea pig genital Ct D infection i.e. day 3 'early' while days 9 and 15 were representative of 'intermediate' post Ct D infection. At days 30 and 65, all animals had cleared the infection (Fig. 1a, late phase of infection). Swab material from Ct D and mock infected animals were subjected to HPLC–MS/MS and metabolite identification using PRISM Data Analysis. Global profiling of lipids detected at five time points of assessment revealed ceramide, triglyceride, sphingomyelin, choline and ethanolamines (Fig. 2). We detected ~2700 species of metabolites across all time points and the belonged to various families as shown in Fig. 2a. Amongst these the largest increase observed was that of PC at 3, 9 and 15 days post infection (section 7, black blowout portion, Fig. 2a–c). However at later time points, triglycerides (TG) were found to be the predominant lipids (Fig. 2d, e). Phosphotidyl-ethanolamine (PE), the precursor of PC exhibited a similar profile, i.e., was observed to be the second most predominant phospholipid detected at 3, 9, and 15 but not 30 and 65 days post infection (Fig. 2a – e). Overall, the observed trend in increases of phospholipid content during active stages of infection and reverting to mock infected levels following clearance of Ct D were indicative of a probable role in infectivity.

3.2 PC 16:0/18:1 and chlamydial infectivity

Considering increased PC content (compared to other lipids) during "active" shedding of organisms in infected animals, i.e. days 3, 9, and 15 concomitant with decreased PC content following 'clearance', i.e., days 30 and 65 (Fig. 2), we investigated the possible contribution of PC in establishment of Ct D infection. Cells (104C1) were infected with Ct D and PC content was assessed by using HPLC–MS/MS. As shown in Fig. 3a, 28 PC species were significantly regulated in vivo (cumulative from all five time point post infection).Amongst these, we found PC 16:0/18:1 to be significantly increased in vitro in 104C1, guinea pig cell line. Ten additional PC species were found to be greater than twofold regulated in Ct D infected cells compared to mock infection (Table 1). While 27 and 10 distinct PC species were detected in vivo and in vitro respectively (Table 1), for our current study we chose to determine the contribution of PC species found to be significantly regulated in both experimental models. PC 16:0/18:1 was regulated in vivo and in vitro following Ct D infection (Fig. 3a; Table 1). As shown in Fig. 3b, following Ct D infection the fold increase in relative ion abundance of PC 16:0/18:1 in infected cells compared to mock infection was 4.52 (in vivo: $p = 0.0137$, 2.04×10^9 compared to 5.5×10^8) and 2.30 (in vitro: $p = 0.0036$, 1.45×10^6 compared to 6.8×10^5). Tocorroborate the findings, we pretreated Hela and 104C1 cells with PC 16:0/18:1 encapsulated liposomes. We found PC 16:0/18:1 encapsulated liposomes to facilitate greater Ct D IFU numbers compared to liposome alone wells in both cell lines (Fig. 3c). Although increase in Ct D IFU were observed in Hela cells

(84 %) and 104C1 (26 %) respectively, it was only statistically significant in Hela cells (p = 0.0016) (Fig. 3c). Taken together, these results suggest that PC 16:0/18:1 may facilitate in vivo and in vitro Ct D infection.

4 Discussion

Intra-vaginal or -cervical Ct infection ascends disproportionately to the upper regions of the genital tract including uterine horns and oviducts (Darville and Hiltke 2010; Rank and Whittum-Hudson 2010; Gondek et al. 2012; Nogueira et al. 2015). Depending on the animal model, a single low-dose Ct inoculation (10^2–10^4) results in vaginal shedding of viable IFUs up to approximately 20–30 days *post* infection with mild to severe inflammation and hydrosalpinx formation, and tubal dilatation in uterine horns and/or oviducts (Morrison and Caldwell 2002; De Clercq et al. 2013; Vanrompay et al. 2005; Igietseme et al. 1998; Pan et al. 2015). Early events in Ct infection including tissue colonization, associated host immune and physiological factors potentially determine the severity and magnitude of ensuing late-stage upper genital pathology (Hafner et al. 2008; Champion et al. 2009; Jiang et al. 2012).

Lipids are integral components of host cellular architecture and critical to structure and function (Fahy et al. 2009; Gross and Han 2011; Subramaniam et al. 2011). It is known that altered lipid metabolism is associated with pathological conditions due to several factors including infection and inflammation (Stubbs and Smith 1984). Although subcellular localization and acquisition of host lipids is extensively known (Hackstadt et al. 1995, 1996; Wylie et al. 1997), the modulation of host lipids following genital Ct and the resultant effect on associated pathological sequelae is not well investigated. Growth and replication of Ct L2 is critically dependent on host derived sphingolipids (van Ooij et al. 2000). Also, *Chlamydia* utilizes Golgi and endoplasmic reticulum associated pathways for acquisition of host lipids including cholesterol and glycerol (Derre 2015; Elwell and Engel 2012; Elwell et al. 2011). Several host Rab GTPases and chlamydial inclusion membrane proteins are involved in lipid accumulation during chlamydial colonization (Capmany and Damiani 2010; Moore et al. 2008; Derre et al. 2011).

Based on the gap on our current understanding and the documented role for lipids in Ct infectivity/colonization, we identified the lipid ‘signatures’ associated with early and late stages of genital Ct D infection in vivo. Using a HPLC–MS/MS approach, the lipidome of Ct D infected guinea pigs at five progressive time points during Ct D infection was determined (Fig. 1). While 13 distinct lipids were abundantly detected across all five time points, PC and precursor molecule, PE were observed to be the most and second-most abundantly detected lipids respectively, amongst all detected metabolites at days 3, 9 and 15 post infection (Fig. 2). Mass spectrometry analyses of PC metabolites revealed significant regulation ($p < 0.05$) of PC 16:0/18:1 in Ct D infected 104C1 cells. Additionally, exogenous addition of PC 16:0/18:1 lead to an increase in Ct D infectivity in Hela 229 and 104C1 cells (Fig. 3c) corroborating our in vivo and in vitro findings (Figs. 2, 3a, b) and indicating a probable role for PC in Ct infection.

PC 16:0/18:1 is a member of phosphatidylcholine synthesized in the liver (Cole et al. 2012). The contribution of PC in modulating bacterial infectivity has been previously implicated-

sterol free PC in the presence of linoleic or arachidonic acid alters *Helicobacter pylori* infectivity (Shimomura et al. 2009). Physiologically, PC significantly contribute to lipoprotein metabolism in inflammatory conditions including non-alcoholic fatty liver disease and cardiovascular disease (de Alwis and Day 2008; Cole et al. 2011). Additionally, PC play a critical role in pulmonary surfactant structure and physiology (Perez-Gil 2008). There is limited information on the role of surfactants in *Chlamydia* biology (Oberley et al. 2004a, b). We have previously reported regulation in pulmonary surfactants at early stages of *C. muridarum* infection in neonatal mice and a mechanistic role in altering structure, function and development of lungs of mice infected at birth (Jupelli et al. 2011). However, the specific role of PC induced changes in surfactants and associated pathology in genital Ct infection needs investigation.

PC 16:0/18:1 has also been reported to be significantly elevated in thyroid papillary and breast cancers and in-term placentas of gestational diabetes patients compared to controls (Ishikawa et al. 2012; Doria et al. 2012; Uhl et al. 2015). While the specific contribution of Ct D to PC 16:0/18:1 is not reported, McClarty and colleagues have demonstrated that Ct L2 accelerates metabolism of PC derived from low density lipoprotein and that endogenous host cell derived PC was trafficked to Ct D inclusions (Hatch and McClarty 2004).

Given that our metabolite results are obtained from endocervical swabs following Ct D infection, the relative contribution of bacteria and the infected host cells/tissues to synthesis and production of these metabolites is unknown. However our results on these host metabolites modulated at stages of Ct infection are associated with infected guinea pigs which are actively shedding recoverable IFUs from the genital tract (Fig. 1a). It is well established that events occurring during host–Ct interactions result in late stage upper genital pathology development (Fig. 2b) (Rey-Ladino et al. 2014). Therefore, our findings provide new insight on host factors that may be important and probably critical to early stage chlamydial infectivity and may potentially influence late stage events. PC 16:0/16:0 and palmitic acid (16:0) is elevated in inflammation, and increase levels of *ICAM-1*, an adhesion molecule in epithelial cells (He et al. 2014; Sanadgol et al. 2012). We have recently established the regulation of an early event-*ICAM-1* via murine microRNA-214 in Ct infected murine genital tract may contribute to late stage upper genital pathology in an IL-17A dependent manner (Arkatkar et al. 2015). Additionally, palmitic acid induces TNF-α and IL-6 (Zhou et al. 2013), cytokines demonstrated by us and others to contribute significantly to causation of upper genital pathology in Ct infected mice (Murthy et al. 2011; Cunningham et al. 2013).

Taken together, these findings indicate that PC induced changes in early stages of infection might potentially contribute to mechanisms that contribute to causation of upper genital pathology. Additionally, our in vivo findings revealed regulation of distinct species of PE, phosphatidyl serines, triglycerides, diacylglycerols and ceramides in Ct D infected guinea pigs compared to mock infection (Supplementary Table S1). Although our present study focuses on the role of PC, the role of these other families of metabolites is warranted. To this end, the reported role of selected metabolites in Ct infection highlights the importance of these species in disease pathogenesis (Szaszak et al. 2013; Hatch and McClarty 2004; Banhart et al. 2014; Muller et al. 2013). Thus overall, the metabolomics approach to

identifying molecules in genital Ct infection hold promise for identification of novel targets for future investigation.

5 Conclusion

In this study, using high-performance liquid chromatography-mass spectrometry, we mapped lipid profiles of female guinea pigs post Ct serovar D intravaginal infection. We found PC to be regulated temporally and to be the predominant metabolite family at early and intermediate stages of infection. Amongst all detected PC species, we observed PC 16:0/18:1 to be significantly regulated in vivo and in vitro following Ct D infection. Exogenesis addition of PC 16:0/18:1 to cells resulted in significant increase in Ct D infection corroborating in vivo association of PC 16:0/18:1 with bacterial burdens in guinea pigs. Taken together, this study demonstrates a role of host metabolites in Ct D infectivity.

Supplementary Material

Refer to Web version on PubMed Central for supplementary material.

Acknowledgments

We thank Dr. Roger Rank (Arkansas Children's Hospital Research Institute) for sharing the 104C1 cell line, his support in establishing the guinea pig model and insightful discussions. We thank Drs. George R. Negrete and Oleg Larionov, Chemistry, UTSA for use of their equipment and reagents to prepare liposome encapsulated PC 16:0/18:1. This work was supported by National Institutes of Health (NIH) Grant (1RO3AI092621-01) and the Center for Excellence in Infection Genomics (CEIG) training Grant (DOD #W911NF-11-1-0136). Partial support of this study was from the Jane and Roland Blumberg Professorship in Biology for Dr. Arulanandam. Mass spectrometry analyses were conducted in the Metabolomics Core Facility of the Mass Spectrometry Laboratory at the University of Texas Health Science Center at San Antonio, with instrumentation funded in part by NIH Grant (1S10RR031586-01).

References

Adekoya N, Truman B, Landen M. Centers for Disease, C., & Prevention. Incidence of notifiable diseases among American Indians/Alaska Natives—United States, 2007–2011. Morbidity and Mortality Weekly Report. 2015; 64(1):16–19. [PubMed: 25590681]

Arkatkar T, Gupta R, Li W, Yu JJ, Wali S, Neal Guentzel M, et al. Murine MicroRNA-214 regulates intracellular adhesion molecule (ICAM1) gene expression in genital Chlamydia muridarum infection. Immunology. 2015; 145(4):534–542. [PubMed: 25865776]

Banhart S, Saied EM, Martini A, Koch S, Aeberhard L, Madela K, et al. Improved plaque assay identifies a novel anti-Chlamydia ceramide derivative with altered intracellular localization. Antimicrobial Agents and Chemotherapy. 2014; 58(9):5537–5546. [PubMed: 25001308]

Brotman RM, Ravel J, Bavoil PM, Gravitt PE, Ghanem KG. Microbiome, sex hormones, and immune responses in the reproductive tract: Challenges for vaccine development against sexually transmitted infections. Vaccine. 2014; 32(14):1543–1552. [PubMed: 24135572]

Brunham RC, Rappuoli R. Chlamydia trachomatis control requires a vaccine. Vaccine. 2013; 31(15): 1892–1897. [PubMed: 23375977]

Capmany A, Damiani MT. Chlamydia trachomatis intercepts Golgi-derived sphingolipids through a Rab14-mediated transport required for bacterial development and replication. PLoS ONE. 2010; 5(11):e14084. [PubMed: 21124879]

Carlson JH, Whitmire WM, Crane DD, Wicke L, Virtaneva K, Sturdevant DE, et al. The Chlamydia trachomatis plasmid is a transcriptional regulator of chromosomal genes and a virulence factor. Infection and Immunity. 2008; 76(6):2273–2283. [PubMed: 18347045]

Champion CI, Kickhoefer VA, Liu G, Moniz RJ, Freed AS, Bergmann LL, et al. A vault nanoparticle vaccine induces protective mucosal immunity. PLoS ONE. 2009; 4(4):e5409. [PubMed: 19404403]

Cole LK, Dolinsky VW, Dyck JR, Vance DE. Impaired phosphatidylcholine biosynthesis reduces atherosclerosis and prevents lipotoxic cardiac dysfunction in ApoE −/− -Mice. Circulation Research. 2011; 108(6):686–694. [PubMed: 21273556]

Cole LK, Vance JE, Vance DE. Phosphatidylcholine biosynthesis and lipoprotein metabolism. Biochimica et Bio-physica Acta. 2012; 1821(5):754–761.

Cruz-Fisher MI, Cheng C, Sun G, Pal S, Teng A, Molina DM, et al. Identification of immunodominant antigens by probing a whole Chlamydia trachomatis open reading frame proteome microarray using sera from immunized mice. Infection and Immunity. 2011; 79(1):246–257. [PubMed: 20956570]

Cunningham K, Stansfield SH, Patel P, Menon S, Kienzle V, Allan JA, et al. The IL-6 response to Chlamydia from primary reproductive epithelial cells is highly variable and may be involved in differential susceptibility to the immunopathological consequences of chlamydial infection. BMC Immunol. 2013; 14:50. [PubMed: 24238294]

Darville T, Hiltke TJ. Pathogenesis of genital tract disease due to Chlamydia trachomatis. Journal of Infectious Diseases. 2010; 201(Suppl 2):S114–S125. [PubMed: 20524234]

de Alwis NM, Day CP. Non-alcoholic fatty liver disease: The mist gradually clears. Journal of Hepatology. 2008; 48(Suppl 1):S104–S112. [PubMed: 18304679]

De Clercq E, Kalmar I, Vanrompay D. Animal models for studying female genital tract infection with Chlamydia trachomatis. Infection and Immunity. 2013; 81(9):3060–3067. [PubMed: 23836817]

de Jonge MI, Keizer SA, El Moussaoui HM, van Dorsten L, Azzawi R, van Zuilekom HI, et al. A novel guinea pig model of Chlamydia trachomatis genital tract infection. Vaccine. 2011; 29(35): 5994–6001. [PubMed: 21718744]

Derre I. Chlamydiae interaction with the endoplasmic reticulum: Contact, function and consequences. Cellular Microbiology. 2015; 17(7):959–966. [PubMed: 25930206]

Derre I, Swiss R, Agaisse H. The lipid transfer protein CERT interacts with the Chlamydia inclusion protein IncD and participates to ER-Chlamydia inclusion membrane contact sites. PLoS Pathogens. 2011; 7(6):E1002092. [PubMed: 21731489]

Derrick T, Roberts C, Rajasekhar M, Burr SE, Joof H, Makalo P, et al. Conjunctival MicroRNA expression in inflammatory trachomatous scarring. PLoS Neglected Tropical Diseases. 2013; 7(3):e2117. [PubMed: 23516655]

Deruaz M, Luster AD. Chemokine-mediated immune responses in the female genital tract mucosa. Immunology and Cell Biology. 2015; 93(4):347–354. [PubMed: 25776842]

Doria ML, Cotrim Z, Macedo B, Simoes C, Domingues P, Helguero L, et al. Lipidomic approach to identify patterns in phospholipid profiles and define class differences in mammary epithelial and breast cancer cells. Breast Cancer Research and Treatment. 2012; 133(2):635–648. [PubMed: 22037781]

Elwell CA, Engel JN. Lipid acquisition by intracellular Chlamydiae. Cellular Microbiology. 2012; 14(7):1010–1018. [PubMed: 22452394]

Elwell CA, Jiang S, Kim JH, Lee A, Wittmann T, Hanada K, et al. Chlamydia trachomatis co-opts GBF1 and CERT to acquire host sphingomyelin for distinct roles during intracellular development. PLoS Pathogens. 2011; 7(9):e1002198. [PubMed: 21909260]

Fahy E, Subramaniam S, Murphy RC, Nishijima M, Raetz CR, Shimizu T, et al. Update of the LIPID MAPS comprehensive classification system for lipids. Journal of Lipid Research. 2009; 50(Suppl):S9–S14. [PubMed: 19098281]

Ferreira R, Borges V, Nunes A, Borrego MJ, Gomes JP. Assessment of the load and transcriptional dynamics of Chlamydia trachomatis plasmid according to strains' tissue tropism. Microbiological Research. 2013; 168(6):333–339. [PubMed: 23590987]

Furuse Y, Finethy R, Saka HA, Xet-Mull AM, Sisk DM, Smith KL, et al. Search for microRNAs expressed by intracellular bacterial pathogens in infected mammalian cells. PLoS ONE. 2014; 9(9):e106434. [PubMed: 25184567]

Gao X, Zhang Q, Meng D, Isaac G, Zhao R, Fillmore TL, et al. A reversed-phase capillary ultra-performance liquid chromatography-mass spectrometry (UPLC-MS) method for comprehensive

top-down/bottom-up lipid profiling. Analytical and Bioanalytical Chemistry. 2012; 402(9):2923–2933. [PubMed: 22354571]

Gondek DC, Olive AJ, Stary G, Starnbach MN. CD4 + T cells are necessary and sufficient to confer protection against Chlamydia trachomatis infection in the murine upper genital tract. J Immunol. 2012; 189(5):2441–2449. [PubMed: 22855710]

Gottlieb SL, Low N, Newman LM, Bolan G, Kamb M, Broutet N. Toward global prevention of sexually transmitted infections (STIs): The need for STI vaccines. Vaccine. 2014; 32(14):1527–1535. [PubMed: 24581979]

Gross RW, Han X. Lipidomics at the interface of structure and function in systems biology. Chemistry & Biology. 2011; 18(3):284–291. [PubMed: 21439472]

Gupta R, Arkatkar T, Yu JJ, Wali S, Haskins WE, Chambers JP, et al. Chlamydia muridarum infection associated host MicroRNAs in the murine genital tract and contribution to generation of host immune response. American Journal of Reproductive Immunology. 2015; 73(2):126–140. [PubMed: 24976530]

Hackstadt T, Rockey DD, Heinzen RA, Scidmore MA. Chlamydia trachomatis interrupts an exocytic pathway to acquire endogenously synthesized sphingomyelin in transit from the Golgi apparatus to the plasma membrane. EMBO Journal. 1996; 15(5):964–977. [PubMed: 8605892]

Hackstadt T, Scidmore MA, Rockey DD. Lipid metabolism in Chlamydia trachomatis-infected cells: Directed trafficking of Golgi-derived sphingolipids to the chlamydial inclusion. Proceedings of the National Academy of Sciences USA. 1995; 92(11):4877–4881.

Hafner LM. Pathogenesis of fallopian tube damage caused by Chlamydia trachomatis infections. Contraception. 2015; 92(2):108–115. [PubMed: 25592078]

Hafner L, Beagley K, Timms P. Chlamydia trachomatis infection: Host immune responses and potential vaccines. Mucosal Immunology. 2008; 1(2):116–130. [PubMed: 19079169]

Hafner LM, Wilson DP, Timms P. Development status and future prospects for a vaccine against Chlamydia trachomatis infection. Vaccine. 2014; 32(14):1563–1571. [PubMed: 23973245]

Hatch GM, McClarty G. C. trachomatis-infection accelerates metabolism of phosphatidylcholine derived from low density lipoprotein but does not affect phosphatidylcholine secretion from hepatocytes. BMC Microbiology. 2004; 4:8. [PubMed: 15018642]

He Q, Takizawa Y, Hayasaka T, Masaki N, Kusama Y, Su J, et al. Increased phosphatidylcholine (16:0/16:0) in the folliculus lymphaticus of Warthin tumor. Analytical and Bioanalytical Chemistry. 2014; 406(24):5815–5825. [PubMed: 24880872]

Huston WM, Harvie M, Mittal A, Timms P, Beagley KW. Vaccination to protect against infection of the female reproductive tract. Expert Review of Clinical Immunology. 2012; 8(1):81–94. [PubMed: 22149343]

Igietseme JU, Omosun Y, Partin J, Goldstein J, He Q, Joseph K, et al. Prevention of Chlamydia-induced infertility by inhibition of local caspase activity. Journal of Infectious Diseases. 2013; 207(7):1095–1104. [PubMed: 23303804]

Igietseme JU, Uriri IM, Kumar SN, Ananaba GA, Ojior OO, Momodu IA, et al. Route of infection that induces a high intensity of gamma interferon-secreting T cells in the genital tract produces optimal protection against Chlamydia trachomatis infection in mice. Infection and Immunity. 1998; 66(9):4030–4035. [PubMed: 9712743]

Ishikawa S, Tateya I, Hayasaka T, Masaki N, Takizawa Y, Ohno S, et al. Increased expression of phosphatidylcholine (16:0/18:1) and (16:0/18:2) in thyroid papillary cancer. PLoS ONE. 2012; 7(11):e48873. [PubMed: 23139822]

Jiang J, Karimi O, Ouburg S, Champion CI, Khurana A, Liu G, et al. Interruption of CXCL13-CXCR5 axis increases upper genital tract pathology and activation of NKT cells following chlamydial genital infection. PLoS ONE. 2012; 7(11):e47487. [PubMed: 23189125]

Jupelli M, Murthy AK, Chaganty BK, Guentzel MN, Selby DM, Vasquez MM, et al. Neonatal chlamydial pneumonia induces altered respiratory structure and function lasting into adult life. Laboratory Investigation. 2011; 91(10):1530–1539. [PubMed: 21769086]

Karunakaran KP, Yu H, Jiang X, Chan Q, Moon KM, Foster LJ, et al. Outer membrane proteins preferentially load MHC class II peptides: Implications for a Chlamydia trachomatis T cell vaccine. Vaccine. 2015; 33(18):2159–2166. [PubMed: 25738816]

Kokes M, Dunn JD, Granek JA, Nguyen BD, Barker JR, Valdivia RH, et al. Integrating chemical mutagenesis and whole-genome sequencing as a platform for forward and reverse genetic analysis of Chlamydia. Cell Host & Microbe. 2015; 17(5):716–725. [PubMed: 25920978]

Lal JA, Malogajski J, Verweij SP, de Boer P, Ambrosino E, Brand A, et al. Chlamydia trachomatis infections and subfertility: Opportunities to translate host pathogen genomic data into public health. Public Health Genomics. 2013; 16(1–2):50–61. [PubMed: 23548718]

Li S, Goins B, Hrycushko BA, Phillips WT, Bao A. Feasibility of eradication of breast cancer cells remaining in postlumpectomy cavity and draining lymph nodes following intracavitary injection of radioactive immunoliposomes. Molecular Pharmaceutics. 2012a; 9(9):2513–2522. [PubMed: 22894603]

Li S, Goins B, Zhang L, Bao A. Novel multifunctional theranostic liposome drug delivery system: Construction, characterization, and multimodality MR, near-infrared fluorescent, and nuclear imaging. Bioconjugate Chemistry. 2012b; 23(6):1322–1332. [PubMed: 22577859]

Li W, Murthy AK, Guentzel MN, Seshu J, Forsthuber TG, Zhong G, et al. Antigen-specific CD4 + T cells produce sufficient IFN-gamma to mediate robust protective immunity against genital Chlamydia muridarum infection. Journal of Immunology. 2008; 180(5):3375–3382.

Li W, Murthy AK, Lanka GK, Chetty SL, Yu JJ, Chambers JP, et al. A T cell epitope-based vaccine protects against chlamydial infection in HLA-DR4 transgenic mice. Vaccine. 2013; 31(48):5722–5728. [PubMed: 24096029]

Lyons JM, Ouburg S, Morre SA. An integrated approach to Chlamydia trachomatis infection: The ICTI Consortium, an update. Drugs of Today. 2009; 45(Suppl B):15–23. [PubMed: 20011690]

Mascellino MT, Boccia P, Oliva A. Immunopathogenesis in Chlamydia trachomatis infected women. ISRN Obstetrics and Gynecol. 2011; 2011:436936.

Mfuh AM, Mahindaratne MP, Quintero MV, Lakner FJ, Bao A, Goins BA, et al. Novel asparagine-derived lipid enhances distearoylphosphatidylcholine bilayer resistance to acidic conditions. Langmuir. 2011; 27(8):4447–4455. [PubMed: 21413760]

Mirrashidi KM, Elwell CA, Verschueren E, Johnson JR, Frando A, Von Dollen J, et al. Global mapping of the inc-human interactome reveals that retromer restricts chlamydia infection. Cell Host & Microbe. 2015; 18(1):109–121. [PubMed: 26118995]

Moore ER, Fischer ER, Mead DJ, Hackstadt T. The chlamydial inclusion preferentially intercepts basolaterally directed sphingomyelin-containing exocytic vacuoles. Traffic. 2008; 9(12):2130–2140. [PubMed: 18778406]

Morrison RP, Caldwell HD. Immunity to murine chlamydial genital infection. Infection and Immunity. 2002; 70(6):2741–2751. [PubMed: 12010958]

Muller C, Dietz I, Tziotis D, Moritz F, Rupp J, Schmitt-Kopplin P. Molecular cartography in acute Chlamydia pneumoniae infections-a non-targeted metabolomics approach. Analytical and Bioanalytical Chemistry. 2013; 405(15):5119–5131. [PubMed: 23354577]

Murthy AK, Li W, Chaganty BK, Kamalakaran S, Guentzel MN, Seshu J, et al. Tumor necrosis factor alpha production from CD8 + T cells mediates oviduct pathological sequelae following primary genital Chlamydia muridarum infection. Infection and Immunity. 2011; 79(7):2928–2935. [PubMed: 21536799]

Neuendorf E, Gajer P, Bowlin AK, Marques PX, Ma B, Yang H, et al. Chlamydia caviae infection alters abundance but not composition of the guinea pig vaginal microbiota. Pathogens and Disease. 2015; 73(4):ftv019. [PubMed: 25761873]

Nogueira CV, Zhang X, Giovannone N, Sennott EL, Starnbach MN. Protective immunity against Chlamydia trachomatis can engage both CD4 + and CD8 + T cells and bridge the respiratory and genital mucosae. Journal of Immunology. 2015; 194(5):2319–2329.

Oberley RE, Ault KA, Neff TL, Khubchandani KR, Crouch EC, Snyder JM. Surfactant proteins A and D enhance the phagocytosis of Chlamydia into THP-1 cells. American Journal of Physiology. Lung Cellular and Molecular Physiology. 2004a; 287(2):L296–L306. [PubMed: 15075250]

Oberley RE, Goss KL, Ault KA, Crouch EC, Snyder JM. Surfactant protein D is present in the human female reproductive tract and inhibits Chlamydia trachomatis infection. Molecular Human Reproduction. 2004b; 10(12):861–870. [PubMed: 15489244]

Owusu-Edusei K Jr, Chesson HW, Gift TL, Brunham RC, Bolan G. Cost-effectiveness of Chlamydia vaccination programs for young women. Emerging Infectious Diseases. 2015; 21(6):960–968. [PubMed: 25989525]

Owusu-Edusei K Jr, Chesson HW, Gift TL, Tao G, Mahajan R, Ocfemia MC, et al. The estimated direct medical cost of selected sexually transmitted infections in the United States, 2008. Sexually Transmitted Diseases. 2013; 40(3):197–201. [PubMed: 23403600]

Ozolins D, D'Elios MM, Lowndes CM, Unemo M, Members of the NCSC. Diagnostics, surveillance and management of sexually transmitted infections in Europe have to be improved: Lessons from the European Conference of National Strategies for Chlamydia trachomatis and Human papillomavirus (NSCP conference) in Latvia, 2011. Journal of the European Academy of Dermatology and Venereology. 2013; 27(10):1308–1311. [PubMed: 22541067]

Pan Q, Pais R, Ohandjo A, He C, He Q, Omosun Y, et al. Comparative evaluation of the protective efficacy of two formulations of a recombinant Chlamydia abortus subunit candidate vaccine in a mouse model. Vaccine. 2015; 33(15):1865–1872. [PubMed: 25698486]

Perez-Gil J. Structure of pulmonary surfactant membranes and films: The role of proteins and lipid-protein interactions. Biochimica et Biophysica Acta. 2008; 1778(7–8):1676–1695. [PubMed: 18515069]

Picard MD, Cohane KP, Gierahn TM, Higgins DE, Flechtner JB. High-throughput proteomic screening identifies Chlamydia trachomatis antigens that are capable of eliciting T cell and antibody responses that provide protection against vaginal challenge. Vaccine. 2012; 30(29):4387–4393. [PubMed: 22682294]

Porcella SF, Carlson JH, Sturdevant DE, Sturdevant GL, Kanakabandi K, Virtaneva K, et al. Transcriptional profiling of human epithelial cells infected with plasmid-bearing and plasmid-deficient Chlamydia trachomatis. Infection and Immunity. 2015; 83(2):534–543. [PubMed: 25404022]

Qu Y, Frazer LC, O'Connell CM, Tarantal AF, Andrews CW Jr, O'Connor SL, et al. Comparable genital tract infection, pathology, and immunity in rhesus macaques inoculated with wild-type or plasmid-deficient Chlamydia trachomatis serovar D. Infection and Immunity. 2015

Rank RG, Bowlin AK, Reed RL, Darville T. Characterization of chlamydial genital infection resulting from sexual transmission from male to female guinea pigs and determination of infectious dose. Infection and Immunity. 2003; 71(11):6148–6154. [PubMed: 14573630]

Rank RG, Whittum-Hudson JA. Protective immunity to chlamydial genital infection: Evidence from animal studies. Journal of Infectious Diseases. 2010; 201(Suppl 2):S168–S177. [PubMed: 20470052]

Rey-Ladino J, Ross AG, Cripps AW. Immunity, immunopathology, and human vaccine development against sexually transmitted Chlamydia trachomatis. Human Vaccines & Immunotherapeutics. 2014; 10(9):2664–2673. [PubMed: 25483666]

Saka HA, Thompson JW, Chen YS, Dubois LG, Haas JT, Moseley A, et al. Chlamydia trachomatis infection leads to defined alterations to the lipid droplet proteome in epithelial cells. PLoS ONE. 2015; 10(4):e0124630. [PubMed: 25909443]

Sanadgol N, Mostafaie A, Mansouri K, Bahrami G. Effect of palmitic acid and linoleic acid on expression of ICAM-1 and VCAM-1 in human bone marrow endothelial cells (HBMECs). Arch Med Sci. 2012; 8(2):192–198. [PubMed: 22661989]

Shimomura H, Hosoda K, Hayashi S, Yokota K, Oguma K, Hirai Y. Steroids mediate resistance to the bactericidal effect of phosphatidylcholines against Helicobacter pylori. FEMS Microbiology Letters. 2009; 301(1):84–94. [PubMed: 19843309]

Sixt BS, Siegl A, Muller C, Watzka M, Wultsch A, Tziotis D, et al. Metabolic features of Protochlamydia amoebophila elementary bodies—A link between activity and infectivity in Chlamydiae. PLoS Pathogens. 2013; 9(8):e1003553. [PubMed: 23950718]

Stubbs CD, Smith AD. The modification of mammalian membrane polyunsaturated fatty acid composition in relation to membrane fluidity and function. Biochimica et Biophysica Acta. 1984; 779(1):89–137. [PubMed: 6229284]

Subramaniam S, Fahy E, Gupta S, Sud M, Byrnes RW, Cotter D, et al. Bioinformatics and systems biology of the lipidome. Chemical Reviews. 2011; 111(10):6452–6490. [PubMed: 21939287]

Szaszak M, Chang JC, Leng W, Rupp J, Ojcius DM, Kelley AM. Characterizing the intracellular distribution of metabolites in intact Chlamydia-infected cells by Raman and two-photon microscopy. Microbes and Infection. 2013; 15(6–7):461–469. [PubMed: 23541981]

Torrone E, Papp J, Weinstock H. Centers for Disease, C., & Prevention. Prevalence of Chlamydia trachomatis genital infection among persons aged 14–39 years—United States, 2007–2012. Morbidity and Mortality Weekly Report. 2014; 63(38):834–838. [PubMed: 25254560]

Uhl O, Demmelmair H, Segura MT, Florido J, Rueda R, Campoy C, et al. Effects of obesity and gestational diabetes mellitus on placental phospholipids. Diabetes Research and Clinical Practice. 2015; 109(2):364–371. [PubMed: 26021978]

van Ooij C, Kalman L, van Ijzendoorn S, Nishijima M, Hanada K, Mostov K, et al. Host cell-derived sphingolipids are required for the intracellular growth of Chlamydia trachomatis. Cellular Microbiology. 2000; 2(6):627–637. [PubMed: 11207614]

Vanrompay D, Hoang TQ, De Vos L, Verminnen K, Harkinezhad T, Chiers K, et al. Specific-pathogen-free pigs as an animal model for studying Chlamydia trachomatis genital infection. Infection and Immunity. 2005; 73(12):8317–8321. [PubMed: 16299329]

Vasilevsky S, Greub G, Nardelli-Haefliger D, Baud D. Genital Chlamydia trachomatis: Understanding the roles of innate and adaptive immunity in vaccine research. Clinical Microbiology Reviews. 2014; 27(2):346–370. [PubMed: 24696438]

Wali S, Gupta R, Veselenak RL, Li Y, Yu JJ, Murthy AK, et al. Use of a Guinea pig-specific transcriptome array for evaluation of protective immunity against genital chlamydial infection following intranasal vaccination in Guinea pigs. PLoS ONE. 2014; 9(12):e114261. [PubMed: 25502875]

Wang J, Zhang Y, Lu C, Lei L, Yu P, Zhong G. A genome-wide profiling of the humoral immune response to Chlamydia trachomatis infection reveals vaccine candidate antigens expressed in humans. Journal of Immunology. 2010; 185(3):1670–1680.

Wylie JL, Hatch GM, McClarty G. Host cell phospholipids are trafficked to and then modified by Chlamydia trachomatis. Journal of Bacteriology. 1997; 179(23):7233–7242. [PubMed: 9393685]

Yeruva L, Myers GS, Spencer N, Creasy HH, Adams NE, Maurelli AT, et al. Early microRNA expression profile as a prognostic biomarker for the development of pelvic inflammatory disease in a mouse model of chlamydial genital infection. MBio. 2014; 5(3):e01241–e01214. [PubMed: 24961692]

Zhou BR, Zhang JA, Zhang Q, Permatasari F, Xu Y, Wu D, et al. Palmitic acid induces production of proinflamma-tory cytokines interleukin-6, interleukin-1beta, and tumor necrosis factor-alpha via a NF-kappaB-dependent mechanism in HaCaT keratinocytes. Mediators of Inflammation. 2013; 2013:530429. [PubMed: 24078775]

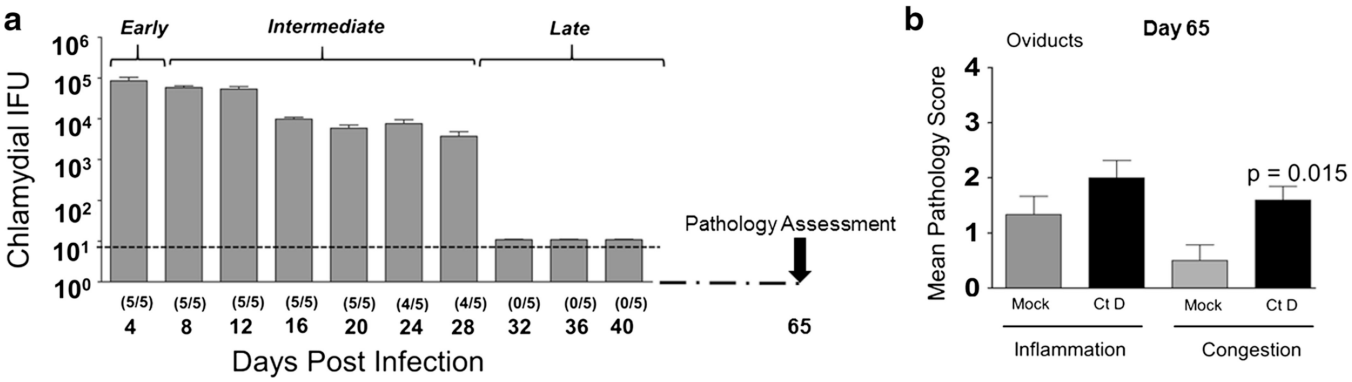

Fig. 1.

Establishment of *Chlamydia trachomatis* serovar D infection in guinea pigs. Guinea pigs (n = 5) were challenged i.vag. with 10^5 IFU Ct D. **a** Chlamydial shedding was monitored every fourth day post infection until day 40 and presented as mean ± SD for each group at each time point. Number of guinea pigs shedding Ct D after genital challenge is indicated in parenthesis. The stages of infection are denoted as early, intermediate and late. **b** Histopathological lesions in genital tracts at day 65 post chlamydial infection. The genital tract of each guinea pig was removed sectioned, H&E stained, and analyzed microscopically. Histopathological injury in the oviducts was scored by two distinct morphological parameters (inflammation cell infiltration and congestion). Significant increase between Ct D infected and mock infected guinea pigs are indicated as calculated using student's *t* test in data of two replicate studies

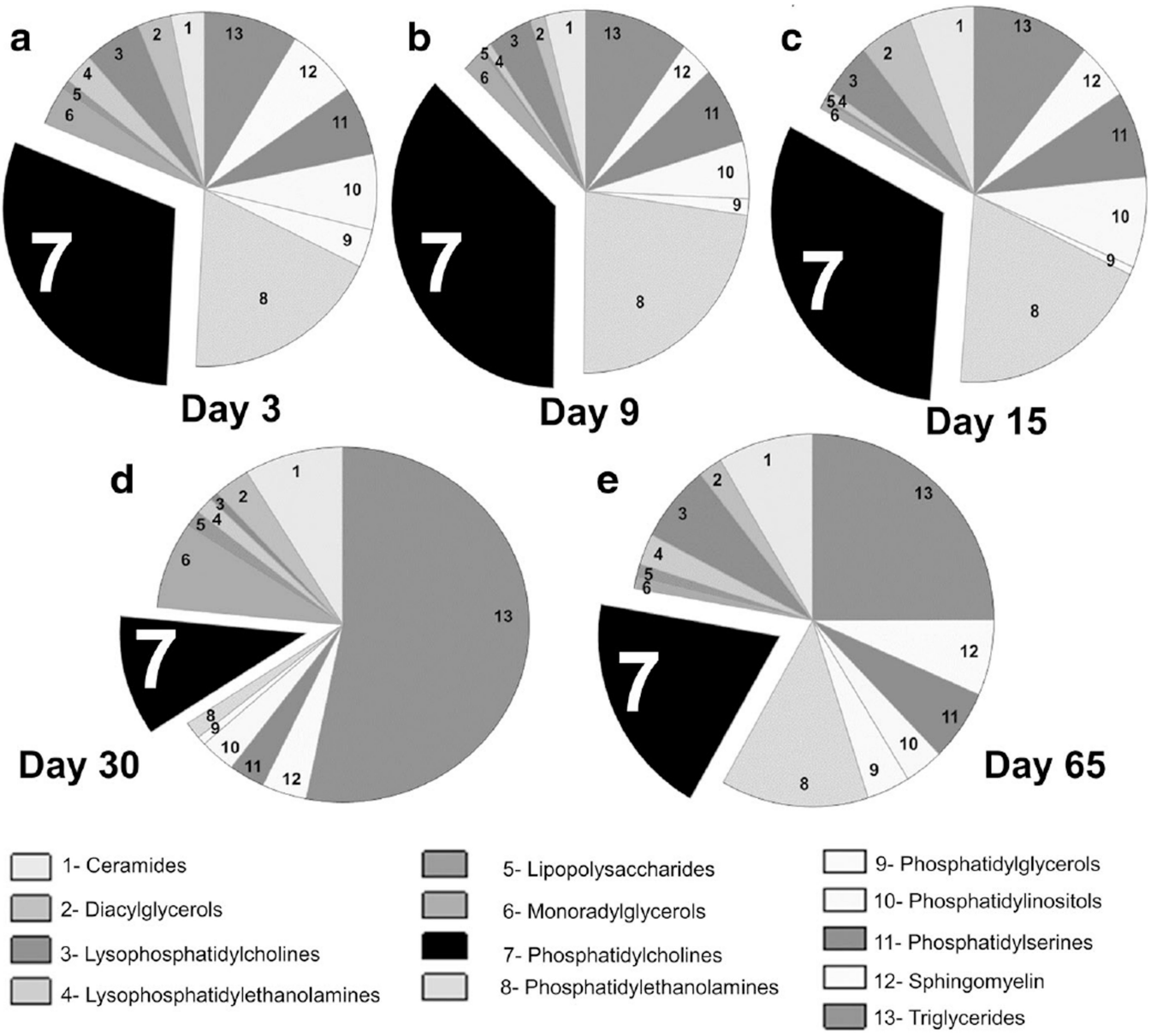

Fig. 2.

Distribution of lipids in Ct D infected guinea pigs. Lipidome profiles of genital swabs collected at early (day 3), intermediate (days 9 and 15) and late (days 30 and 65) time points post Ct D infection were determined. Using HPLC–MS/MS, the most abundantly detected lipids were annotated according to the PRISM Data Analysis system. Pie chart representation of Ct D infected lipids to have >twofold abundance in Ct D infected compared to mock infected guinea pigs. The blow-out section (black, section 7) represents the phosphatidyl choline which were observed to be most abundant during infection. Significant increase between Ct D infected and mock infected guinea pigs are indicated as calculated using student's *t* test in data from 1 of 2 replicates as mean ± SD

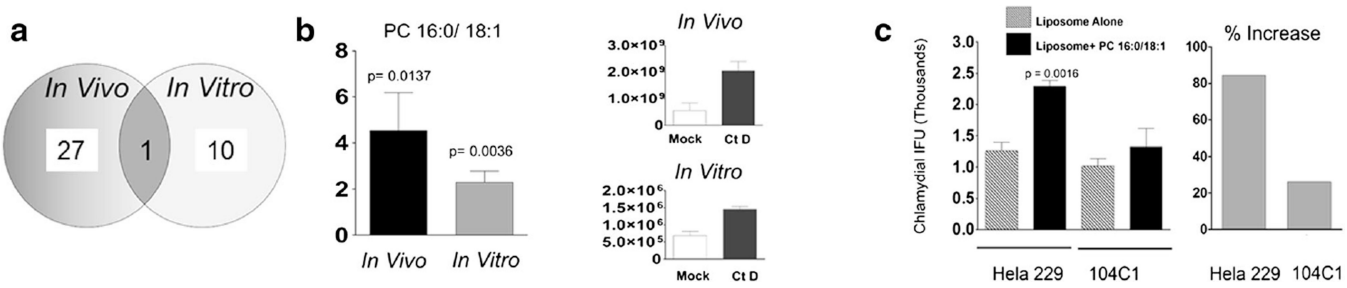

Fig. 3.

Role of phosphatidyl choline 16:0/18:1 in Ct D infection. **a** Venn diagram representation of PC species with >twofold increase in Ct D infection compared to mock infection. *Numbers in each circle* denote total number of PC in vivo (guinea pig swabs) and in vitro (104C1 guinea pig cell line). Phosphatidyl choline 16:0/18:1 was observed to be statistically significant and >twofold in both groups and indicated in the overlapping area. **b** Relative fold change of PC 16:0/18:1 in guinea pigs (in vivo) and 104C1 (in vitro) and total abundance. **c** Increase in Ct D IFUs in Hela (human cell line) and 104C1 cells following exogenous addition of PC 16:0/18:1 encapsulated liposomes. Significant increase between Ct D infected and mock infected cells are indicated as calculated using student's *t* test in data from 1 of 3 replicates as mean ± SD

Table 1

Fold changes in phosphatidyl choline (PC) following *Chlamydia trachomatis* D infection (A) In vivo (swabs obtained from guinea pigs) and (B) In Vitro (104C1, a guinea pig cell line)

(A) In vivo			(B) In vitro		
PC	**FC[a]**	**Ion abundance[b]**	**PC**	**FC[a]**	**Ion abundance[b]**
PC(16:0/19:0) + H	7.53	2.2×10^8 vs 2.9×10^7	PC(16:1/13:0) + H	8.10	6.3×10^7 vs 7.8×10^6
PC(16:0/22:1) + H	2.78	1.0×10^9 vs 3.8×10^8	PC(16:0/18:2) + H	17.45	2.1×10^{10} vs 1.2×10^9
PC(16:0/18:1) + H	4.52	2.0×10^9 vs 5.5×10^8	PC(16:0/18:1) + H	2.30	1.5×10^6 vs 6.8×10^5
PC(16:0e/15:0) + H	3.73	8.3×10^8 vs 2.2×10^8	PC(18:0/18:2) + H	8.72	2.4×10^6 vs 2.8×10^5
PC(16:0e/16:0) + H	4.93	4.3×10^9 vs 8.8×10^8	PC(18:0/18:1) + H	7.28	1.5×10^6 vs 2.1×10^5
PC(16:0p/24:2) + H	8.78	1.4×10^9 vs 1.6×10^8	PC(16:0p/22:6) + H	25.13	3.4×10^8 vs 1.3×10^7
PC(16:1/19:1) + H	8.62	6.4×10^7 vs 7.4×10^6	PC(17:1/20:4) + H	13.63	1.3×10^8 vs 9.2×10^6
PC(16:1p/24:2) + H	10.52	8.1×10^8 vs 7.7×10^7	PC(17:0/20:4) + H	18.34	3.4×10^8 vs 1.9×10^7
PC(18:0/16:0) + H	5.59	2.2×10^9 vs 4.08×10^8	PC(18:0/20:4) + H	25.81	2.5×10^9 vs 9.7×10^7
PC(18:0/18:1) + H	2.88	1.6×10^{10} vs 5.6×10^9	PC(16:1/24:7) + H	14.45	2.3×10^8 vs 1.6×10^7
PC(18:0e/20:4) + H	2.86	1.71×10^9 vs 5.9×10^8	PC(20:0/19:0) + H	8.28	5.9×10^7 vs 7.1 9 10^6
PC(18:0p/19:1) + H	3.00	4.9×10^8 vs 1.6×10^8			
PC(18:1/20:4) + H	6.44	9.4×10^8 vs 1.4×10^8			
PC(18:1p/24:2) + H	10.51	4.5×10^8 vs 4.3×10^7			
PC(20:0/22:4) + H	2.69	1.5×10^8 vs 5.6×10^7			
PC(18:1p/15:0) + H	2.76	4.6×10^8 vs 1.7×10^8			
PC(16:0/22:6) + H	7.98	4.9×10^8 vs 6.2×10^7			
PC(16:0e/15:0) + H	5.00	4.4×10^8 vs 8.8×10^7			
PC(16:0e/18:1) + H	5.97	6.3×10^9 vs 1.0×10^9			
PC(16:0e/20:4) + H	2.71	8.4×10^8 vs 3.1×10^8			
PC(16:1/18:2) + H	6.54	2.2×10^9 vs 3.4×10^8			
PC(16:1/19:1) + H	6.55	2.9×10^7 vs 4.4×10^6			
PC(18:0/16:0) + H	6.92	1.6×10^9 vs 2.4×10^8			
PC(18:0/18:1) + H	2.58	1.1×10^{10} vs 4.3×10^9			
PC(18:0e/16:0) + H	2.88	5.1×10^5 vs 1.7×10^5			

(A) In vivo			(B) In vitro		
PC	**FC[a]**	**Ion abundance[b]**	**PC**	**FC[a]**	**Ion abundance[b]**
PC(18:0p/18:2) + H	5.40	9.0×10^9 vs 1.8×10^9			
PC(18:0p/20:4) + H	2.95	7.6 × 108 vs 2.6 × 108			
PC(19:1/18:2) + H	3.85	4.2 × 108 vs 1.1 × 108			

[a] Fold change (FC) was calculated as ratio of ion abundance (A) in swab collected from Ct D infected to mock infected swab at respective time point; (B) Ct D infected/mock infected cells

[b] Ion abundance was plotted as values obtained in Ct D infected group compared to mock infected groups. vs versus